Corrosion Behavior of Spark Plasma Sintered Alumina and Al$_2$O$_3$-SiC-CNT Hybrid Nanocomposite

Z.H. Al-Ashwan[a], U. Hayat[a], I.H. Toor[a], Syed Fida Hassan[a], N. Saheb[a,b]*

[a] *King Fahd University of Petroleum and Minerals, Department of Mechanical Engineering, Dhahran, Saudi Arabia*
[b] *King Fahd University of Petroleum and Minerals, Centre of Research Excellence in Nanotechnology, Dhahran 31261, Saudi Arabia*

The use of ceramic-based materials has become more common in many applications because of their unique characteristics and properties. Design of alumina hybrid nanocomposites achieved by incorporating two nanoreinforcements, with different morphologies and/or attributes, such as CNTs and SiC, is a new approach that has been adopted to enhance the properties of alumina. The microstructural, mechanical, electrical, and thermal properties of Al$_2$O$_3$-SiC-CNT hybrid nanocomposites were investigated and reported in the literature. However, the corrosion behavior was not considered. The present paper reports the electrochemical corrosion behavior of pure Al$_2$O$_3$ and Al$_2$O$_3$-5SiC-2CNT hybrid nanocomposite in acidic (2.34M HCl) and alkaline (6.5M NaOH) environments at room temperature. Ball milling (BM) and spark plasma sintering (SPS) were used for preparation of samples. The microstructure of sintered samples was investigated through field emission scanning electron microscopy (FE-SEM). Potentiodynamic polarization (PDP) technique was used to investigate the corrosion behavior. The corrosion rate of the Al$_2$O$_3$-5SiC-2CNT nanocomposite increased 96 and 178% in HCl and NaOH solution, respectively, compared to alumina. Possible corrosion mechanisms and factors effecting corrosion were discussed.

Keywords: *Alumina, hybrid ceramic nanocomposites, spark plasma sintering, electrochemical corrosion.*

1. Introduction

Alumina is the most widely used and studied ceramic because of its good mechanical properties, high temperature stability, wear and corrosion resistance, along with electrical and thermal insulation nature[1,2]. Due to these properties, alumina is widely used in applications involving critical conditions[3], such as high pressure, temperature and corrosive environments, i-e in cutting tools, dental implants, gas laser turbines, high temperature bearings, mechanical seals in nuclear reactors, and wear resistant parts[1,4-8]. Lower fracture toughness is the only restraint[1,9], restricting the use of alumina in wide range of applications. In order to overcome this limitation, micro/nano sized reinforcements such as CNT, CNF, SiC, and graphene are added to alumina matrix[10-12], resulting in the formation of nanocomposites with improved fracture toughness[13]. Recently, further enhancements in properties of alumina were made possible through the hybrid microstructural design[14], by reinforcing alumina with two reinforcements simultaneously. For instance, 117% increase in fracture toughness along with 44% increase in bending strength was reported by Ahmad and Pan[14], for Al$_2$O$_3$-SiC-CNT hybrid nanocomposites in comparison to monolithic alumina.

Generally, ceramics are known for their good corrosion resistance[15]. However, they are susceptible to corrosion in presence of corrosive environment. In case of monolithic alumina, corrosion investigations under different corrosive environments such as hydrothermal[4,16], acidic[3,17-20] and alkaline[21,22] media were reported. Oda and Yoshio[4] investigated hydrothermal corrosion at 300°C and 8.6 MPa pressure, using alumina with variable purity levels (99%, 99.9% and 99.99%), for 1 to 10 days. The authors observed intergranular corrosion and attributed it to the dissolution of grain-boundary impurities, which was confirmed from the presence of Si, Na, and Al ions in the solution. The corrosion weight loss and resulting strength, of the corroded samples, were found to be dependent on purity level, with the highly pure sample showing the lowest corrosion and highest strength. Ono et al.[16] and Sato et al.[21], in similar investigations, showed the dependency of corrosion on the purity of alumina. The 92% alumina sample showed higher corrosion rate of 3.48 mg/cm^3, as compared to 0.145 mg/cm^3 of the 99.5% alumina sample, in demineralized water at 275°C after 100 hours of exposure[16]. Schacht[18] investigated corrosive attack of various acids on alumina within temperature range of up to 500°C. High purity alumina was found more corrosion resistant. Also, it was reported that corrosive attack of acids decrease in order of; H$_3$PO$_4$ > H$_2$SO$_4$ > HCl. In another study, Genthe et al.[19] reported the corrosion behaviors of alumina doped with MgO, Y$_2$O$_3$, Cr$_2$O$_3$, ZrO$_2$, BaO, and

*email: nouari@kfupm.edu.sa

SiO_2 in different acidic (H_3PO_4, H_2SO_4, HNO_3, HF, HCl) and alkaline (NaOH) media within a low temperature range of up to 180°C. Lidija et al.[20] studied the effect of different concentrations (2, 10 and 20wt.%) of HCl and H_2SO_4 on corrosion behavior of alumina. Corrosive attack on alumina was found decreasing with increased acidic concentrations. However, in case of alkaline caustic solution, an opposite trend of increased corrosive attack with increase in concentration of NaOH was reported by Sato[21]. All these studies suggest that corrosion attack starts from grain boundaries, by the dissolution of grain boundary impurities. It was found that the intensity of corrosion attack depends on the purity of alumina, nature and concentration of the corrosive media, time of exposure, and temperature of the medium.

With growing applications of alumina, especially in the fields of biomaterials and bio-pharmaceuticals[23-25], efforts were made to enhance the corrosion resistance of alumina while enhancing or retaining the other properties. Shikha et al.[23] reported the enhancement of corrosion resistance of alumina through surface modification using N^+ ions implantation at 60 keV. Corrosion current density (i_{corr}) of the un-implanted alumina was found to be 4.62 $\mu A/cm^2$ in Ringer solution, this was reduced to 1.11 $\mu A/cm^2$ for the sample implanted with ion beam dose of 1×10^{16} ions/cm^2. Also, nanohardness was found to increase from 10 to 37.5 GPa, when alumina was implanted with N^+ beam dose of 1×10^{16} ions/cm^2. This enhancement in corrosion resistance and nanohardness was attributed to the formation of hard AlN and AlON compounds on the surface of the implanted sample. Wu et al.[4] reported that addition of Y_2O_3 in alumina led to increased corrosion resistance in 12 wt% HCl +3 wt% HF acid, due to the formation of $Y_3Al_5O_{12}$ and $CaAl_{12}O_{19}$ acid resistant phases within alumina. Lekatou et al.[25] studied the corrosion and tribological properties of alumina reinforced with 0-50wt.%Ni in 3.5wt.% NaCl. Both corrosion and wear rate of the reinforced alumina decreased, as compared to pure alumina, up to 30wt.% of Ni reinforcement.

It was reported that the addition of reinforcements alter the mechanical, electrical, thermal and corrosion behavior of alumina. Literature is available on mechanical[26-33], electrical[34-39] and thermal[39-44] behavior of alumina-based nanocomposites. However, corrosion behavior of alumina hybrid nanocomposites was not considered. Due to the fact that alumina-based-nanocomposites are mostly designed for applications with extreme working conditions, knowledge of corrosion behavior is equally important. In previous works, the authors investigated the effect of SiC and CNT reinforcement on microstructural and mechanical properties[45] as well as electrical and thermal properties[39] of Al_2O_3-SiC-CNT hybrid nanocomposites. In this work, the effect of SiC and CNT on corrosion behavior of spark plasma sintered alumina was investigated in both acidic and alkaline media, using potentiodynamic polarization method. Corrosion mechanism was discussed, corrosion rates were calculated and factors effecting corrosion behavior were explained.

2. Materials and Methods

Pure alumina powder, having 99.85% purity (particle size of 150 nm), procured from ChemPUR Germany; SiC_β (45–55nm) with 97.5% purity supplied by Nanostructured and Amorphous Material and locally manufactured functionalized carbon nanotubes (CNTs), produced through chemical vapour deposition (CVD) were used in this study. The hybrid nanocomposite was synthesized via two stages. In the first stage, Al_2O_3-10Si nanocomposite powder was prepared by sonication and ball milling. In the second stage, the required amount of functionalized CNTS was added to the slurry and further sonicated for 2 h using a high-energy probe sonicator to obtain Al_2O_3-10SiC-2CNT nanocomposite. Pure Al_2O_3 and Al_2O_3-5SiC-2CNT samples were sintered through spark plasma sintering (SPS) at 1500°C for 10 minutes holding time. Detailed methodology for nanocomposite powder preparation and sintering is explained somewhere else[39,45]. Disc shaped specimens (a diameter of 20 mm and a height of 10 mm) were prepared using a graphite die. Tescan Lyra-3 FE-SEM was used to analyze the microstructure of spark plasma sintered samples.

Corrosion testing was conducted at room temperature (25°C), within electrochemical three-electrode cell. The tested specimen was used as working electrode. A platinum wire and a saturated calomel electrode (SCE) were used as counter and reference electrodes, respectively. Detailed working of the polarization cell is can be found in the literature[46]. Gamry potentiostat (Reference 3000) was used for potentiodynamic polarization. Samples were ground and polished prior to corrosion testing. A special 3M tape with an exposed working area of 0.22 cm^2 was used on specimen surface. Electrochemical testing was conducted in both acidic (2.34 mol/l HCl) and alkaline (6.5 mol/l NaOH) solution mediums, using a scan rate of 0.2 mV/s. In built software of potentiostat, DC105, was used to interpret the Tafel region of potentiodynamic curves and to determine the values of corrosion potential (E_{corr}), corrosion current (i_{corr}), and corrosion rate.

3. Results and Discussion

Figure 1 shows FE-SEM images of surfaces of Al_2O_3 and Al_2O_3-5SiC-2CNT nanocomposite samples. The black arrows show CNTs. Reduction in grain size of alumina due to addition of SiC and CNT reinforcements can be observed. This reduction in grain size, also reported by Saheb and Khwaja[45], is primarily due to the pinning effect of the reinforcements, which restricts the grain boundary motion during densification[11]. The mode of fracture changed from intergranular for pure alumina to intragranular for Al_2O_3-5SiC-2CNT nanocomposite. These mechanisms of grain refinement and change of fracture mode are few important factors contributing towards enhanced mechanical properties of Al_2O_3-SiC-CNT nanocomposites[14,45].

The potentiodynamic polarization response of Al_2O_3 and Al_2O_3-5SiC-2CNT hybrid nanocomposite in 2.34M HCl and 6.5M NaOH solutions is shown in Figure 2. The curves of Al_2O_3-5SiC-2CNT nanocomposite are present towards higher current density, in both acidic and alkaline solutions, showing relatively high corrosion as compared to monolithic alumina. Table 1 shows the values of corrosion parameters of Al_2O_3 and Al_2O_3-5SiC-2CNT nanocomposite in 2.34 M HCl and 6.5M NaOH solutions. In the case of HCl solution, corrosion rate and i_{corr} of pure alumina were found to be 5.07 x 10^{-3} mpy and 1.12 nA that increased to
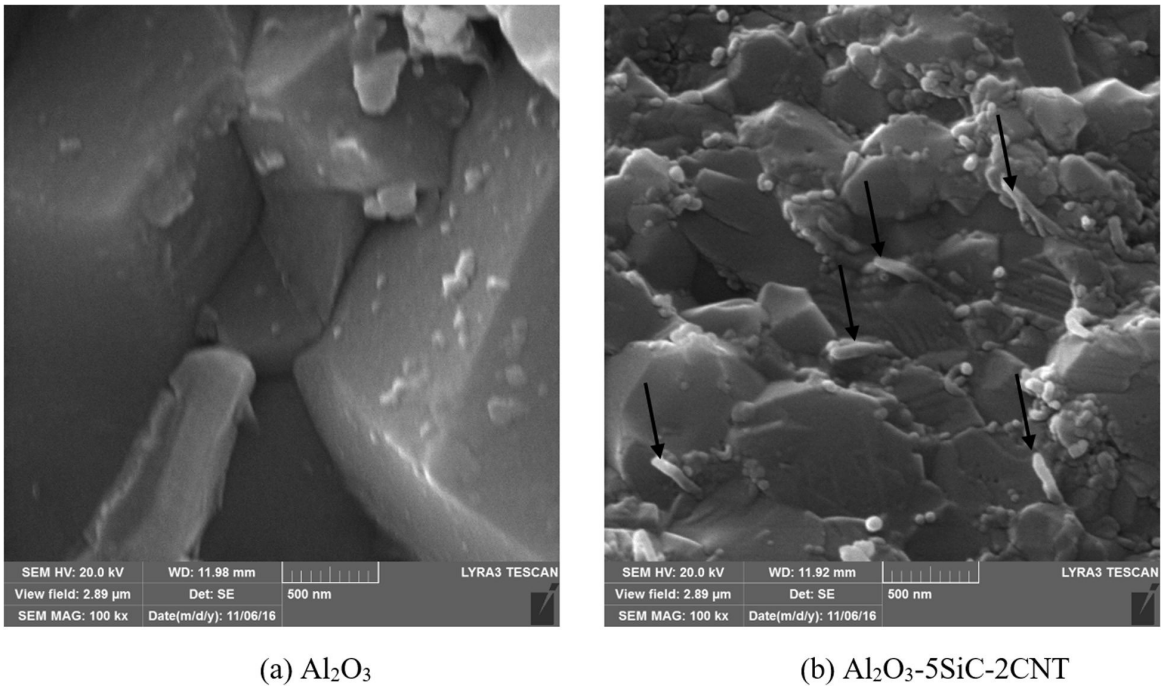
(a) Al$_2$O$_3$

(b) Al$_2$O$_3$-5SiC-2CNT

Figure 1: FE-SEM images of surfaces of Al$_2$O$_3$ and Al$_2$O$_3$-5SiC-2CNT nanocomposite samples.
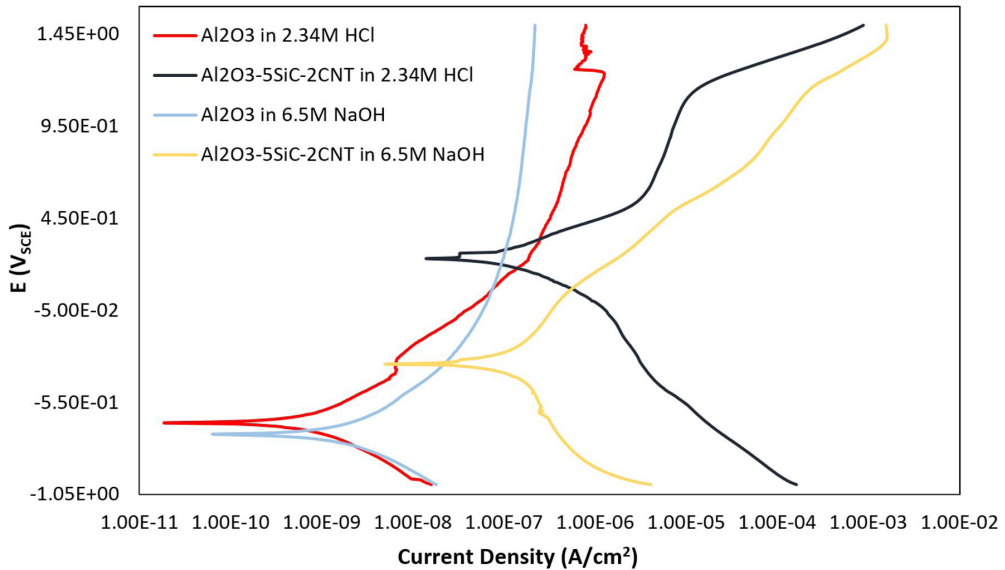
Figure 2: Potentiodynamic polarization response of Al$_2$O$_3$ and Al$_2$O$_3$-5SiC-2CNT hybrid nanocomposite.

0.488 mpy and 105 nA for Al$_2$O$_3$-5SiC-2CNT nanocomposite, respectively. Similarly, in case of NaOH solution, corrosion rate and i$_{corr}$ of pure alumina increased from 12.8×10^{-3} mpy and 2.82 nA to 2.282 mpy and 494 nA for Al$_2$O$_3$-5SiC-2CNT nanocomposite. This clearly shows that the addition of SiC and CNT to alumina increased its corrosion in both acidic and alkaline environments.

Corrosion results of Al$_2$O$_3$ and Al$_2$O$_3$-5SiC-2CNT nanocomposite in acidic and alkaline environments, presented in Table 1, shows that corrosion in 6.5 M NaOH alkaline solution was severe as compared to 2.34 M HCl solution. This is due to the fact that acids are more corrosive at lower concentrations[20], while alkaline bases are more corrosive at higher concentrations[21]. For example, an increase in corrosive attack of HCl and H$_2$SO$_4$ on alumina was observed by Lidija et al[.0], when concentrations of acids were reduced from 20 to 2 wt.%. Also, in the case of NaOH alkaline solution, the increase in the corrosion of alumina with increase in concentration from 0.1 to 25 M of NaOH, was reported by Sato and coworkers[21].

Table 1. Summary of potentiodynamic polarization data for spark plasma sintered Al_2O_3 and Al_2O_3-5SiC-2CNT hybrid nanocomposite in HCl and NaOH solutions

	2.34 mol/l HCl		6.5 mol/l NaOH	
	Al_2O_3	Al_2O_3-5SiC-2CNT	Al_2O_3	Al_2O_3-5SiC-2CNT
E_{corr} (mV$_{SCE}$)	-659	235	-725	-345
I_{corr} (nA)	1.12	105	2.82	494
Corrosion Rate (mpy*)	5.07×10^{-3}	0.488	12.8×10^{-3}	2.282

*mils per year

Oda and Yoshio [4] reported that corrosion in alumina is generally intergranular in nature, where corrosive attack starts preferentially on grain boundaries, resulting in dissolution of SiO_2 and NO_2 grain boundary impurities. Other researcher[20] attributed the corrosion of alumina, in HCl and H_2SO_4 acid solutions, to the dissolution of MgO, Na_2O, CaO, SiO_2 and Fe_2O_3 grain boundary impurities. This intergranular nature of corrosive attack in alumina has also been reported in other studies[3,21,22]. Due to the fact that grain boundaries are the high energy sites, they are more susceptible to corrosive attack. For instance, Mikeska et al.[3] found that single-crystal alumina had higher corrosion resistance than polycrystalline alumina in aqueous hydrofluoric acid. After corrosive dissolution of grain boundaries, grains get exposed to corrosive media and eventually they wash out of the sample[18]. Hence, corrosion resistance in alumina is primarily dependent on microstructure and impurities present within grain boundaries[19]. It is believed that in the case of Al_2O_3-5SiC-2CNT nanocomposite, the presence of large number of grain boundaries due to grain refinement, Figure 1, the increased number of interfaces, and possible agglomeration of the reinforcements have contributed to corrosive attack. Similar behavior of increased corrosion with increase in reinforcement content was reported by Lekatou et al.[25] for sintered alumina-Ni nanocomposites. The authors found that, in 3.5wt.% NaCl solution, the corrosion current density value of 0.89 mA/cm^2 for pure alumina increased to 2.52 and 2.44 mA/cm^2 for Al_2O_3-40wt.%Ni and Al_2O_3-50wt.%Ni nanocomposites, respectively. This increased corrosion current density, in case of Al_2O_3-Ni nanocomposites, was attributed to Ni agglomeration, increase in grain boundaries and increased number of interfaces. Moreover, corrosion in alumina is highly sensitive to impurities present within grain boundaries[4]. SiC and CNTs in the nanocomposite behave like impurities and increases the corrosion rate. Influence of impurity content on corrosion behavior of alumina has been reported by Oda and Yoshio [4]. The authors found that alumina with 99% purity suffered relatively higher corrosion, as compared to alumina with 99.9% purity. In another similar study[16], sintered alumina with 99.5% purity displayed higher corrosion resistance, in demineralized water at 275°C, compared to alumina with 92% purity. The corrosion rates of 92 and 99.5% alumina were found to be 3.48 and 0.145 mg/cm^3, respectively.

Corrosion behavior is known to depend on the electrical conductivity of the material[47]. Due to its electrical insulating nature, corrosion of alumina is generally attributed to chemical corrosive attack[24]. For the Al_2O_3-5SiC-2CNT nanocomposite, addition of SiC and CNT resulted in the formation of interconnected network of semiconducting phases within the grain boundaries of alumina, which enhanced the electrical conductivity. An electrical conductivity of 8.85 S/m was reported for Al_2O_3-5SiC-2CNT nanocomposite[39], as compared to 6.87×10^{-10} S/m for alumina. The high electrical conductivity provided more electronic flow during polarization, resulting in intensifying the corrosive attack of the electrolyte, thus increasing the corrosion of Al_2O_3-5SiC-2CNT nanocomposite. Similar behavior was overserved by Sydow et al[8] in their investigation on two types of SiC ceramics with different electrical resistivity values. They found that SiC with high electrical conductivity showed high corrosion. Also, Liu and co-authors [49], reported corrosion current densities of 0.70 and 0.82 mA/cm^2, for alumina nanocomposite containing 0.33 wt.% carbon, in 1M HCl and 1M NaOH solutions, respectively. The increase in carbon content to 0.62 and 0.82 wt.% resulted in increased corrosion. This increase in corrosion rate was attributed to the increase in the electrical conductivity due to the formation of nano-carbon interconnected network within alumina grain boundaries.

It is known that alumina with relatively low porosity is more resistant to corrosive attack[18]. Therefore, the presence of small fraction of porosity in Al_2O_3-5SiC-2CNT nanocomposite might have contributed towards high corrosion. The pure alumina used in this study was almost fully dense (99.8%), while the Al_2O_3-5SiC-2CNT nanocomposite had 97.2% relative density[39]. Because of porosity, relatively larger interface area of Al_2O_3-5SiC-2CNT nanocomposite was exposed to the electrolyte, as compared to alumina, resulting in higher corrosion. However, because of the very low porosity in Al_2O_3-5SiC-2CNT nanocomposite, it is believed that its contribution in increasing corrosion, if any, is very small. It is worth mentioning here that in their investigation on the corrosion behavior of MgO-doped alumina, with different MgO contents in acidic solutions (HCl, H_2SO_4, HNO_3), Genthe and Hausner[19] concluded that porosity and composition of grain boundaries are defining factors for corrosion behavior. This influence was also observed by Oda and Yoshio[4], where high purity alumina with relatively high density showed more corrosion resistance as compared to less pure alumina with low density.

The corrosion behavior of metal matrix composites and nanocomposites has been thoroughly investigated and reported[50-54], however, it was not considered for hybrid ceramic matrix nanocomposites. Therefore, the corrosion rates of the alumina and Al_2O_3-5SiC-2CNT nanocomposite samples were compared with those of some metals and metal matrix nanocomposites[50,55-61] and presented in Table 2. It can be clearly seen that the Al_2O_3 and Al_2O_3-5SiC-2CNT nanocomposite have relatively low corrosion rates. It is worth mentioning here that although the Al_2O_3-5SiC-2CNT

Table 2. Corrosion rates of different metals, alloys and metal-matrix nanocomposites

Materials	Corrosive environment	Corrosion rate (mpy)	Ref.
Al_2O_3	2.34 mol/l HCl*	5.07×10^{-3}	this work
Al_2O_3	6.5 mol/l NaOH	12.8×10^{-3}	this work
$Al_2O_3$5SiC-2CNT*	2.34 mol/l HCl*	0.488	this work
$Al_2O_3$5SiC-2CNT	6.5 mol/l NaOH*	2.282	this work
Fe	1N HCl	92080	50
Mg	3M MgCl$_2$	12×10^3	55
Mg	3.5wt.% NaCl	2499	56
AA*7075	3.5wt.% NaCl	4.25	57
AA6061-T6	3.5wt.% NaCl	4.433	58
Al 6061	3.5wt.% NaCl	25	59
Cu-30%Zn (Brass)	3.5wt.% NaCl	0.3029	60
Fe-10%Al_2O_3	1N HCl	3878	50
Mg-0.1%GNP	3.5wt.% NaCl	1048	56
Mg-0.5%GNP		2090	
AA 7075+1%CNT	3.5wt.% NaCl	14.71	57
AA 7075+1%CNT		20.99	
Al 6061-10%SiC	3.5wt.% NaCl	35.86	59
Al 6061-10%SiC		72.24	
Al7075+2.5%SiC+2.5%TiC	3.5wt.% NaCl	2.505	61
Al 7075+5%SiC+5%TiC		1.235	

*AA (Aluminium Alloy)

nanocomposite showed higher corrosion rate than alumina, its corrosion resistance remained high compared with many metals and metal matrix nanocomposites. This corrosion behavior coupled with mechanical[45] as well as electrical and thermal properties[39] make these alumina hybrid nanocomposites potential materials in many applications such as cutting tools, dental implants, chemical and electrical insulators, and armouries[62].

4. Conclusion

The corrosion behavior of spark plasma sintered alumina and Al₂O₃-5SiC-2CNT hybrid nanocomposite, in acidic and alkaline conditions, was investigated. From this work, the authors concluded the following:

(1) The Al₂O₃-5SiC-2CNT hybrid nanocomposite had a higher corrosion rate than pure alumina in both acidic and alkaline solutions.

(2) In the HCl solution, the corrosion rates of pure alumina and Al₂O₃-5SiC-2CNT nanocomposite were 5.07×10^{-3} and 0.488 mpy, respectively.

(3) In the NaOH solution, the corrosion rates of pure alumina and Al₂O₃-5SiC-2CNT nanocomposite were 12.8×10^{-3} and 2.282 mpy, respectively.

(4) The high corrosion rate of Al₂O₃-5SiC-2CNT hybrid nanocomposite was attributed to the increased number of grain boundaries due to grain refinement, presence of impurities on grain boundaries, and increased electrical conductivity of the nanocomposite.

Acknowledgments

References

1. Ighodaro OL, Okoli OI. Fracture toughness enhancement for alumina systems: a review. Int J Appl Ceram Technol. 2008;5:313-23.
2. Munro R. Evaluated material properties for a sintered alpha-Alumina. J Am Ceram Soc. 1997;80:1919-28.
3. Mikeska KR, Bennison SJ, Grise SL. Corrosion of ceramics in aqueous hydrofluoric acid. J Am Ceram Soc. 2000;83:1160-4.
4. Oda K, Yoshio T. Hydrothermal corrosion of alumina ceramics. J Am Ceram Soc. 1997;80:3233-6.
5. Jack D. Ceramic cutting tool materials. Mater Des. 1986;7:267-73.
6. Geric K. Ceramics tool materials with alumina matrix. TIC. 2010;200:310-410.
7. Chakraborty A, Ray K, Bhaduri S. Comparative wear behavior of ceramic and carbide tools during high speed machining of steel. Mater Manuf Process. 2000;15:269-300.
8. Al-Sanabani FA, Madfa AA, Al-Qudaimi NH. Alumina ceramic for dental applications: a review article. Amer J Mater Res. 2014;1:26-34.
9. Ćurković L, Rede V, Grilec K, Mulabdić A. Hardness and fracture toughness of alumina ceramics. In: 12th Conference on Materials, Processes Friction and Wear, 21-23 June 2007; Vela Luka. Proceedings. Vela Luka, Croatia: Croatian Society for Materials and Tribology; 2007. p. 40-5.
10. Sarkar S, Das PK. Processing and properties of carbon nanotube/alumina nanocomposites: a review. Rev Adv Mater Sci. 2014;37:53-82.
11. Galusek D, Galusková D. Alumina matrix composites with non-oxide nanoparticle addition and enhanced functionalities. Nanomaterials (Basel). 2015;5:115-43.
12. Camargo PHC, Satyanarayana KG, Wypych F. Nanocomposites: synthesis, structure, properties and new application opportunities. Mater Res. 2009;12:1-39.
13. Choi S-M, Awaji H. Nanocomposites: a new material design concept. Sci Technol Adv Mater. 2005;6:2-10.
14. Ahmad K, Pan W. Hybrid nanocomposites: a new route towards tougher alumina ceramics. Compos Sci Technol. 2008;68:1321-7.

15. Tuurna S, Nikkilä A-P, Mäntylä TA. Corrosion resistance of porous alumina ceramics in acetic acid solution. Key Eng Mater, 2002, 206-213(213):1923-1926.

16. Ono S, Suzuki K, Kumagai M, Hoashi K. Corrosion and Elution Behaviors of Al2O3 Ceramics in High-Temperature Demineralized Water. Zairyo-to-Kankyo. 1991;40:655-60.

17. Ćurković L, Kurajica S, Jelača MF, Marinković M. Corrosion behaviour alumina ceramics in aqueous HCl solution. In: 12th Conference on Materials, Processes Friction and Wear, 21-23 June 2007; Vela Luka. Proceedings. Vela Luka, Croatia: Croatian Society for Materials and Tribology, 2007.

18. Schacht M, Boukis N, Dinjus E. Corrosion of alumina ceramics in acidic aqueous solutions at high temperatures and pressures. J Mater Sci. 2000;35:6251-8.

19. Genthe W, Hausner H. Influence of chemical composition on corrosion of alumina in acids and caustic solutions. J Eur Ceram Soc. 1992;9:417-25.

20. Ćurković L, Jelača MF, Kurajica S. Corrosion behavior of alumina ceramics in aqueous HCl and H2SO4 solutions. Corros Sci. 2008;50:872-8.

21. Sato T, Sato S, Okuwaki A, Tanaka Si. Corrosion behavior of alumina ceramics in caustic alkaline solutions at high temperatures. J Am Ceram Soc. 1991;74:3081-4.

22. Galusková D, Hnatko M, Galusek D, Šajgalík P. Corrosion of Structural Ceramics Under Sub-Critical Conditions in Aqueous Sodium Chloride Solution and in Deionized Water. Part II: Dissolution of Al2O3-Based Ceramics. J Am Ceram Soc. 2011;94:3044-52.

23. Shikha D, Jha U, Sinha S, Barhai P, Kalavathy S, Nair K, et al. Improvement in corrosion resistance of biomaterial alumina after 60 keV nitrogen ion implantation. Int J Appl Ceram Technol. 2008;5:44-8.

24. Wu T, Zhou J, Wu B. Effect of Y2O3 on acid resistance of alumina ceramic. Ceram Int. 2017;43:5102-7.

25. Lekatou A, Kenanoglou I, Kalantzis K, Karantzalis A, Sioulas D. Surface degradation of composites prepared by Al2O3 and Ni Nanopowders," Mater Sci Eng Adv Res. 2017;Spe Issue:7-18.

26. Ahmad I, Unwin M, Cao H, Chen H, Zhao H, Kennedy A, et al. Multi-walled carbon nanotubes reinforced Al 2 O 3 nanocomposites: mechanical properties and interfacial investigations. Compos Sci Technol. 2010;70:1199-206.

27. Bi S, Hou G, Su X, Zhang Y, Guo F. Mechanical properties and oxidation resistance of α-alumina/multi-walled carbon nanotube composite ceramics. Mater Sci Eng A. 2011;528:1596-601.

28. Borrell A, Alvarez I, Torrecillas R, Rocha VG, Fernández A. Microstructural design for mechanical and electrical properties of spark plasma sintered Al2O3–SiC nanocomposites. Mater Sci Eng A. 2012;534:693-8.

29. Deng Z-Y, Shi J-L, Zhang Y-F, Jiang D-Y, Guo J-K. Pinning effect of SiC particles on mechanical properties of Al2O3–SiC ceramic matrix composites. J Eur Ceram Soc. 1998;18:501-8.

30. Fei Y, Huang C, Liu H, Zou B. Mechanical properties of Al2O3–TiC–TiN ceramic tool materials. Ceram Int. 2014;40:10205-9.

31. Lee K, Mo CB, Park SB, Hong SH. Mechanical and electrical properties of multiwalled CNT-Alumina nanocomposites prepared by a sequential two-step processing of ultrasonic spray pyrolysis and spark plasma sintering. J Am Ceram Soc. 2011;94:3774-9.

32. Parchovianský M, Galusek D, Sedláček J, Švančárek P, Kašiarová M, Dusza J, et al. Microstructure and mechanical properties of hot pressed Al2O3/SiC nanocomposites. J Eur Ceram Soc. 2013;33:2291-8.

33. Shi X, Xu F, Zhang Z, Dong Y, Tan Y, Wang L, et al. Mechanical properties of hot-pressed Al2O3/SiC composites. Mater Sci Eng A. 2010;527:4646-9.

34. Ahmad K, Pan W. Dramatic effect of multiwalled carbon nanotubes on the electrical properties of alumina based ceramic nanocomposites. Compos Sci Technol. 2009;69:1016-21.

35. Ahmad K, Pan W, Shi S-L. Electrical conductivity and dielectric properties of multiwalled carbon nanotube and alumina composites. Appl Phys Lett. 2006;89:3122.

36. Inam F, Yan H, Jayaseelan DD, Peijs T, Reece MJ. Electrically conductive alumina–carbon nanocomposites prepared by spark plasma sintering. J Eur Ceram Soc. 2010;30:153-7.

37. Kumari L, Zhang T, Du G, Li W, Wang Q, Datye A, et al. Synthesis, microstructure and electrical conductivity of carbon nanotube–alumina nanocomposites. Ceram Int. 2009;35:1775-81.

38. Parchovianský M, Galusek D, Švančárek P, Sedláček J, Šajgalík P. Thermal behavior, electrical conductivity and microstructure of hot pressed Al2O3/SiC nanocomposites. Ceram Int. 2014;40:14421-9.

39. Saheb N, Hayat U. Electrical conductivity and thermal properties of spark plasma sintered Al2O3-SiC-CNT hybrid nanocomposites. Ceram Int. 2017;43:5715-22.

40. Ahmad K, Pan W, Wan CL. Electro-mechanical and thermal properties of multiwalled carbon nanotube reinforced alumina composites, Key Eng Mater, 2008;363:701-03.

41. Ahmad K, Wei P, Wan C. Thermal conductivities of alumina-based multiwall carbon nanotube ceramic composites. J Mater Sci. 2014;49:6048-55.

42. Barea R, Belmonte M, Osendi I, Miranzo P. Thermal conductivity of Al2O3/SiC platelet composites. J Eur Ceram Soc. 2003;23:1773-8.

43. Chu K, Jia C, Tian W, Liang X, Chen H, Guo H. Thermal conductivity of spark plasma sintering consolidated SiC p/Al composites containing pores: numerical study and experimental validation. Compos, Part A Appl Sci Manuf. 2010;41:161-7.

44. Kumari L, Zhang T, Du G, Li W, Wang Q, Datye A, et al. Thermal properties of CNT-Alumina nanocomposites. Compos Sci Technol. 2008;68:2178-83.

45. Saheb N, Mohammad K. Microstructure and mechanical properties of spark plasma sintered Al2O3-SiC-CNTs hybrid nanocomposites. Ceram Int. 2016

46. Stansbury EE, Buchanan RA. Fundamentals of electrochemical corrosion: Materials Park, OH: ASM international; 2000.

47. Herrmann M, Sempf K, Schneider M, Sydow U, Kremmer K, Michaelis A. Electrochemical corrosion of silicon carbide ceramics in H2SO4. J Eur Ceram Soc. 2014;34:229-35.

48. Sydow U, Schneider M, Herrmann M, Kleebe HJ, Michaelis A. Electrochemical corrosion of silicon carbide ceramics: Part 1: Electrochemical investigation of sintered silicon carbide (SSiC). Materials and Corrosion. 2010;61(8), 657-64.

49. Liu J, Menchavez RL, Watanabe H, Fuji M, Takahashi M. Highly conductive alumina/NCN composites electrodes fabricated by gelcasting and reduction-sintering: an electrochemical behavior study in aggressive environments. Electrochim Acta. 2008;53:7191-7.

50. Gupta P, Kumar D, Quraishi M, Parkash O. Effect of sintering parameters on the corrosion characteristics of iron-alumina metal matrix nanocomposites. Journal of Materials and Environmental Science. 2015;6:155-67.

51. Gupta P, Kumar D, Quraishi MA, Parkash O. Effect of cobalt oxide doping on the corrosion behavior of iron-alumina metal matrix nanocomposites. Adv Sci Eng Med. 2013;5(12):1279-91.

52. Gupta P, Kumar D, Quraishi MA, Parkash O. Influence of processing parameters on corrosion behavior of metal matrix nanocomposites. J. Mater. Env. Sci. 2016;7(7):2505-12.

53. Khosla P, Singh HK, Katoch V, Dubey A, Singh N, Kumar D, et al. Synthesis, mechanical and corrosion behaviour of iron–silicon carbide metal matrix nanocomposites. J Compos Mater. 2018;52(1):91-107.

54. Jamwal A, Prakash P, Kumar D, Singh N, Sadasivuni KK, Harshit K, et al. Microstructure, wear and corrosion characteristics of Cu matrix reinforced SiC–graphite hybrid composites. J Compos Mater. 2019;53(18):2545-53.

55. Cramer SD, Covino B. ASM Handbook Vol. 13 A Corrosion: Fundamentals, Testing, and Protection. Materials Park, OH: ASM International; 2003.

56. Turan ME, Sun Y, Akgul Y, Turen Y, Ahlatci H. The effect of GNPs on wear and corrosion behaviors of pure magnesium. J Alloys Compd. 2017;724:14-23.

57. Thirumaran SNB, Kumaresh SP. Corrosion behaviour of CNT reinforced AA 7075 nanocomposites. Adv Mater. 2013;2:1-5.

58. Hussian HA, Hassan KS, Ismeal MK. Corrosion Behavior of Nanocomposite Al-9 wt% Si Alloy Reinforced with Carbon Nanotubes. Al-Khwarizmi Engineering Journal. 2017;13:66-73.

59. Abbass MK, Hassan KS, Alwan AS. Study of corrosion resistance of aluminum alloy 6061/SiC composites in 3.5% NaCl solution. International Journal of Materials, Mechanics and Manufacturing. 2015;3:31-5.

60. Almomani MA, Nemrat MH. Effect of silicon carbide addition on the corrosion behavior of powder metallurgy Cu30Zn brass in a 3.5 wt% NaCl solution. J Alloys Compd. 2016;679:104-14.

61. Sambathkumar M, Navaneethakrishnan P, Ponappa K, Sasikumar K. Mechanical and corrosion behavior of Al7075 (Hybrid) metal matrix composites by two step stir casting process. Lat Am J Solids Struct. 2017;14:243-55.

62. Saheb N, Hayat U, Hassan SF. Recent Advances and Future Prospects in Spark Plasma Sintered Alumina Hybrid Nanocomposites. Nanomaterials (Basel). 2019;9(11):1607.